DELFT UNIVERSITY OF TECHNOLOGY

FACULTY OF AEROSPACE ENGINEERING

AE4870B

RE-ENTRY SYSTEMS

# Assignment III: Ballistic Flight

Lecturer: Dr. E. Mooij

Hours spent: 3.5h

December 9, 2022

Lorenz Veithen 5075211

Delft University of Technology

# 1 Sensitivity to Atmospheric Model

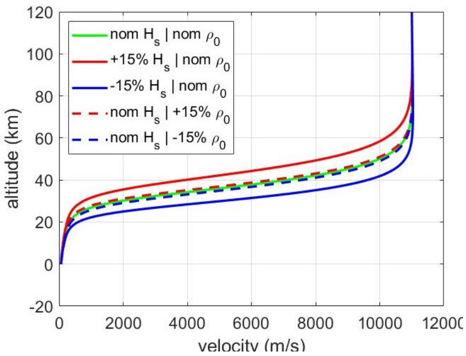


Figure 1: Effect of $H_s$ and $\rho_0$ variations on the trajectory of the Apollo capsule model.

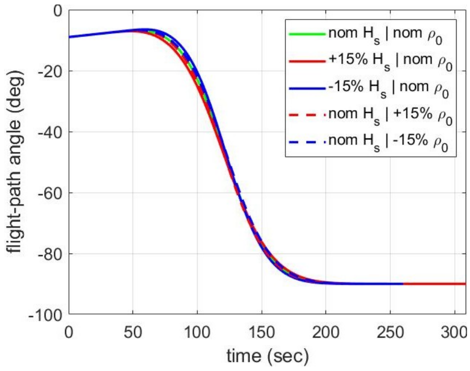


Figure 2: $\gamma_E$ as a function of time for different variations of scale height $H_s$ and reference density $\rho_0$.

As was seen in assignment I, an exponential atmosphere model can be tailored to the US76 model by minimising the relative difference between the two models, by fitting the scale height $H_s$ and density at the reference altitude $\rho_0$. This was done in two steps: first, the least square method was used to find initialisation values into feed to a non-linear solver, then the minimisation of $d\rho = (\rho_{ref} - \rho_0 e^{\frac{h}{H_s}})/(\rho_{ref})$ was performed using the *fmincon* function from MATLAB to solve the non-linear optimisation problem. This resulted in $H_s = 6.9265e + 03$ m and $\rho_0 = 1.5035$ kg/m$^3$, which will be used as nominal values in the subsequent analysis. Varying both parameters by 15% one after the other, yields changes in the trajectory of the entry vehicle, as shown by Figure 1, where the following conventions are applied: dashed lines indicate a change in one variable, and continuous lines in the other ($\rho_0$ and $H_s$ respectively here); red indicates an increase in the variable and blue a decrease in the variable; green indicates the 'nominal' condition. Considering the trajectory from Figure 1, the following can be noted:

- It can first be seen that the effect of the scale height variation has a much larger impact on the altitude-velocity profile than that of $\rho_0$. This was already seen from assignment I, where $H_s$ had the largest influence in the magnitude of the density at higher altitudes (by changing the slope in the logarithmic scales), while changes in $\rho_0$ can be seen as a shift in the density profile of the atmosphere. This can be further understood from the analytical model derived in class, given by Equation (1), where the contribution of the scale height is both in the exponential and as a scaling factor (and those contributions do not cancel each other), when considering the logarithmic scale of $\frac{V}{V_E}$. Essentially $H_s$ drives the atmosphere's relative structure (very significant) while $\rho_0$ fixes the structure to an initial value (less significant).

$$ln\left(\frac{V}{V_E}\right) = \frac{H_s g \rho_0 e^{-h/H_s}}{2K sin(\gamma_E)} \tag{1}$$

- Due to the different nature of the contributions of $\rho_0$ and $H_s$ to the model, the effect of the variation on the shape of the curves in Figure 1 is essentially different: up to some extent (at the limit points), variations in $\rho_0$ seem to conserve the same shape, by (only) scaling the nominal curve up or down (which come from the idea that $\rho_0$ scales the structure of the atmosphere to the surface level value); while variations in $H_s$ change the shape of the trajectory especially at the start and end of the deceleration. Additionally, it can be seen that a larger scale height results in a smoother deceleration, which happens on a larger range of altitudes. That is the case because the variation in density on an altitude difference $\Delta h$ is smaller for a larger scale height, resulting in a more distributed deceleration than for lower scale heights where the deceleration is more concentrated towards the lower layers of the atmosphere.
- All trajectories start the entry in a free fall, until the drag becomes significant enough to decelerate the vehicle effectively. The deceleration starts earlier for the red curves (in Figure 1) which represent atmospheres with a larger density at high altitudes. This can be explained using the simple analytical model derived in class, as seen in Equation (1). A larger $\rho_0$ and/or $H_s$ causes an earlier drop in velocity with respect to the entry velocity. The opposite is true for lower values of those parameters.
- Following, as already hinted from the start of the trajectory discussion, an increase in either of the two base parameters results in the main part of the deceleration occurring at higher altitudes, hence prior to the relatively denser parts of the atmosphere. This is explained by exactly the same argument as mentioned in the previous point. This results in the vehicle being slower in the relatively denser parts of the atmosphere.

Furthermore, the impact on the flight path angle can be considered through Figure 2, which shows that only a slight variation in the way the flight path angle varies over time arises for different values of $H_s$ and $\rho_0$. Furthermore, it is interesting to note that the general behaviour shows that all the horizontal velocity of the vehicle is zeroed by the drag over time, meaning that the end of the trajectory happens in a pure vertical motion.

These variations in the trajectory, and in the structure of the atmosphere, have a direct effect on the thermo-mechanical loads experienced by the vehicle. Typical curves for the g-load and heat flux consist of a $\approx$bell curve with a peak at a specific altitude, for a maximum value of the studied variable. Those peaks (of $q_c$ and $a/g$) generally occur at different altitudes. However, it is desirable to have the largest possible altitude difference between those two points to

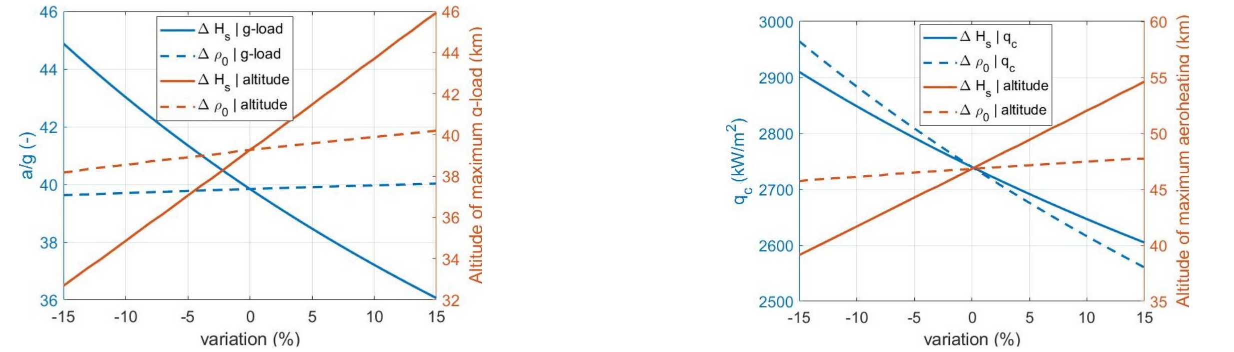


(a) Maximum g-load and its related altitude.

(b) Maximum aerothermal heating and its related altitude.

Figure 3: Variation of maximum g-load and aerothermal heating during entry, and their related altitude, from a $\pm 15\%$ variation of $\rho_0$ and $H_s$.

avoid the maximum g-load to occur shortly after the structure was weakened by the high temperatures associated to the peak in heat flux. Figure 3 provides the value of those peaks and their altitude for the g-load (Figure 3a) and the heat flux (Figure 3b) cases, for variations of the exponential atmosphere parameters by 15%.

First considering Figure 3a, which shows the maximum g-load values in blue and their related altitude in orange:

- It can first be seen that the maximum g-load value is rather independent of $\rho_0$, as was derived in the simplified analytical model, which predicted the maximum acceleration from Equation (2). Though, a very slight variation can be seen, it is negligible and might be due to higher order effects. On the other hand, the altitude at which the maximum g-load occurs has a direct relation with $\rho_0$: a higher value of the latter gives the same density profile shifted to higher altitudes (by $\ln(\rho_0)$ according to the analytical model), meaning that the same loads occur at higher altitudes. This can also be seen from the analytical model, from Equation (3).

$$\bar{a}_{max} = \frac{sin(\gamma_E)}{2H_s e} V_E^2 \qquad (2)$$

$$h' = H_s ln\left(\frac{-\rho_0 g H_s}{K sin(\gamma_E)}\right) \qquad (3)$$

- Furthermore, it can be seen that the influence of the scale height is much more significant, as can be seen from the $\bar{a}_{max}$ formula from the analytical model. An increase in $H_s$ results in a decrease in the maximum g-load experienced by the vehicle. This is the result of a higher density at higher altitudes, which causes the vehicle to lose more energy in the initial parts of the entry, meaning that a lower velocity is reached in the denser parts of the atmosphere, resulting in a lower maximum g-load. This is directly linked to the earlier observation that the deceleration is smoother for a larger scale height, as the vehicle starts its deceleration earlier. Additionally, it is directly seen that the altitude of highest g-load increases for larger $H_s$, which makes sense from the previous discussion that the main part of the deceleration occurs at higher altitudes for a larger scale height (due to the larger densities at higher altitudes).

Second, the thermal flux experienced by the vehicle can be investigated from Figure 3b:

- Both an increase in scale height and reference density result in a decrease in the heat flux experienced by the vehicle. For the former, a similar reasoning to the decrease in maximum g-load can be applied: the energy of the vehicle is dissipated on a larger altitude range, resulting in a smaller peak. The effect of $\rho_0$ is then essentially the same, as larger densities are experienced through the entire atmosphere compared to the nominal case; meaning that the higher layers cause the vehicle to lose more energy than in the nominal case. Therefore, less energy is to be dissipated in the lower layers, where a maximum of $q_c$ is reached.
- The altitude of the variation due to the change in $\rho_0$ is essentially the same as for the g-load case. This can be explained from the analytical model which relates the altitude of the maximum thermal (h") flux to the altitude of the maximum g-load (h') with Equation (4) (with $n = 0.5$ for laminar flows), which is independent of $\rho_0$. Similarly, the same trend as the maximum g-load altitude is found for a variation in scale height. However, the difference in altitude with the maximum g-load point is larger for larger $H_s$, as predicted by the aforementioned analytical model (about 6 km for -15% and 9km for +15%).

$$h'' - h' = -H_s \ln(\frac{2}{3}(1-n)) \qquad (4)$$

From this section, it can be concluded that the accuracy of the atmospheric model used is very important when it is used for the design of a re-entry vehicle, especially considering the points of maximum g-load and thermal flux. On the one hand, an accurate estimate of $\rho_0$ is especially important for the thermal design of the vehicle, as it has the largest influence on the maximum thermal flux experienced during the flight, but its influence on the maximum g-load and the overall trajectory is relatively negligible. On the other hand, the $H_s$ needs to be known very accurately due to its large influence on the trajectory, g-load and thermal flux. This has a direct influence on the estimated landing location (from the trajectory), and on the structural and thermal design. Particularly, the scale height has a large influence on the altitude difference between the point of maximum thermal flux and the point of maximum g-load, which needs to be accurately known due to the change in material properties of the structure from the thermal flux.

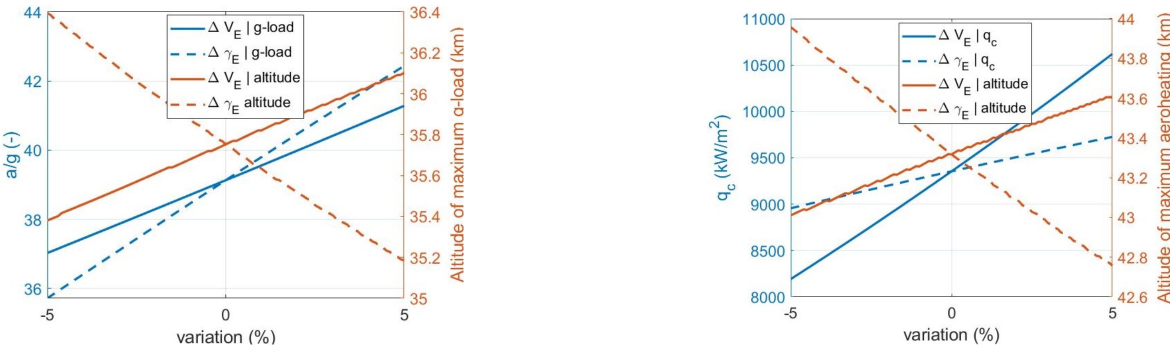


(a) Maximum g-load and its related altitude.

(b) Maximum aeroheating and its related altitude.

Figure 4: Variation of maximum g-load and aeroheating during entry, and their related altitude, from a $\pm 5\%$ variation of $V_E$ and $\gamma_E$.

## 2 Sensitivity to Entry Conditions

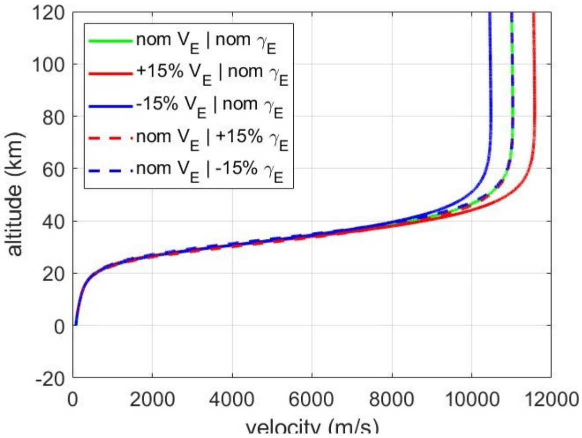


Figure 5: Altitude-velocity curves for 15% variation of $V_E$ and $\gamma_E$.

From this section onwards, the entry vehicle geometry generated in assignment II, with a nose radius $R_N = 0.7$ m, semi-cone angle $\theta_c = 35.7°$, and a base radius $r_{c_2} = 1.5$ m, will be used (for a mass of 2500 kg). Its aerodynamic properties for an angle of attack of 0°(and therefore $C_L = 0$) were generated and loaded in the solver. In the following, the influence of the entry conditions (velocity $V_E$ and flight path angle $\gamma_E$) on the thermo-mechanical loads is considered by investigating a variation of 5% of those parameters. Figure 4 presents the results of this sensitivity analysis. Note that the nominal atmospheric parameters from the previous section are used in the following, and that the small wobbles on the lines are due to numerical errors. Additionally, the nominal values are $V_E = 11$ km/s and $\gamma_E = 9°$.

First considering the effect of a variation in the entry velocity, it can be seen that a larger maximum g-load and maximum thermal flux will result from an increase in $V_E$. This is explained by the fact that the vehicle has more energy to dissipate through the flight, for the same atmospheric conditions (meaning that the start of the deceleration occurs only at a slightly higher altitude than in the nominal case). Figure 5 provides more insight in the flight profile with different entry velocities. It can clearly be seen that despite significantly different $V_E$'s, the altitude-velocity profile quite quickly converge to each other, due to the different dynamic pressures (and hence drag, larger for larger entry velocity) they are subject to. The different drag forces that are acting in the early flight profile of each configuration are at the source of this difference in $a/g$ and $q_c$: higher entry velocities are subject to higher dynamic pressures and drag (higher g-load), meaning that the vehicle loses more energy (which translates to a larger thermal flux). This is also confirmed by the description of the analytical model, given by Equations (2) and (5). Note that comparing Figures 4a and 4b, the relative increase of $q_c$ is larger than the relative increase of $a/g$, which is consistent with the analytical model. Following, the altitude of the maximum in g-load and thermal flux also increase for increasing entry velocities. This can be explained from the fact that at higher velocities, a smaller density (higher altitude) is required to obtain the same dynamic pressure and hence drag, which generally shifts up the thermo-mechanical loads profiles. However, this increase in the altitude of the maximum $q_c$ and $a/g$ is quite small ($\approx 2\%$ at most), as also shown by the analytical model shown by Equations (3) and (4), which are independent of $V_E$.

$$q_{c,max} = c_1 V_E^3 \sqrt{-\frac{K sin(\gamma_E)}{3e R_N g H_s}} \tag{5}$$

Secondly, the effect of varying the entry flight path angle is considered. Increasing the flight path angle results in a trajectory which is more 'vertical' and therefore dives quicker into the atmosphere. An increase in $\gamma_E$ therefore results in less time (and distance) to decelerate the spacecraft prior to its arrival in the denser lower layers of the atmosphere. This results in a larger dynamic pressure and therefore drag acting on the vehicle, than if the trajectory had been shallower, for the same altitude. This larger drag increases both the maximum g-load and the thermal flux on the vehicle. This results in changes in $q_c$ and $a/g$ as shown by Figure 4, and is also reflected through the linear dependence of those parameters on $sin(\gamma_E)$ in the analytical model given by Equations (2) and (5). Furthermore, the altitude of the maximum g-load and thermal flux decrease with increasing entry flight angle, which is also explained from the reasoning above: the $a/g$ and $q_c$ at higher altitudes is not smaller than in the nominal case, but the maximum is reached at a lower altitude as the velocity of the vehicle is higher than the nominal case at lower, denser altitudes.

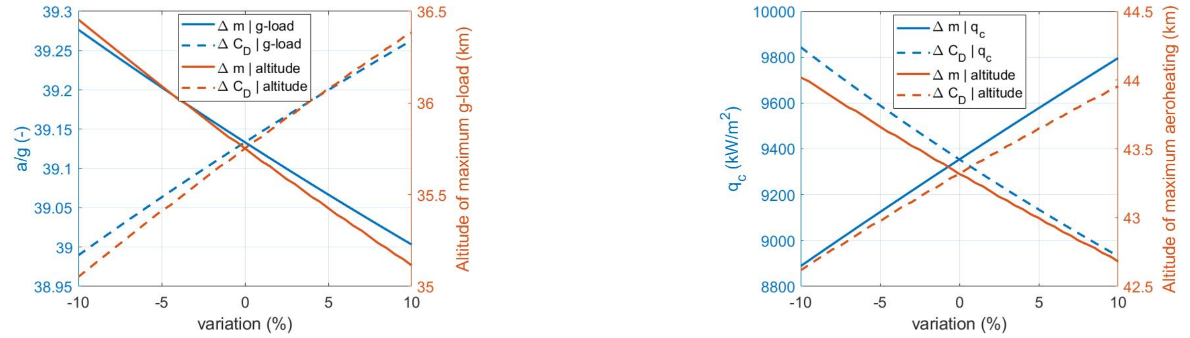


(a) Maximum g-load and its related altitude.

(b) Maximum aeroheating and its related altitude.

Figure 6: Variation of maximum g-load and aeroheating during entry, and their related altitude, from a $\pm 10\%$ variation of $m$ and $C_D$.

From this analysis, it can be concluded that it is desired to enter the atmosphere at lower velocities and flight path angles in order to reduce the g-load and thermal fluxes on the vehicle. However, decreasing the initial velocity of the entry requires special care in the decommissioning of the satellite to be able to reduce the orbital velocity right at the moment of entering the atmosphere. Further note that a smaller $\gamma_E$ results in a larger range covered during the ballistic flight, which carries more uncertainty about the exact landing site location. Furthermore, changes in the difference in altitude between the points of maximum $q_c$ and $a/g$, due to changes in $V_E$ and $\gamma_E$, are generally negligible (as described by the analytical model from Equation 4).

## 3 Sensitivity to the Mass and Drag Coefficient

In this section, the effect of the mass and drag coefficient of the vehicle on the thermo-mechanical loads will be investigated by varying each by 10% one after the other. The vehicle described in the previous section will be used, with a nominal mass of 2500 kg and the drag coefficient computed using the Modified Newtonian Flow model from assignment II (for $\alpha = 0°$). Note that varying those parameters comes back to varying the ballistic coefficient $K = \frac{mg}{C_D S}$. The results of this analysis can be seen in Figure 6.

First considering the g-load on the vehicle, it can be seen that an increase in drag coefficient, or a decrease in mass results in an increase in the maximum deceleration. On a first order, this makes sense as a larger $C_D$ results in a larger drag force and therefore acceleration for the same mass; and a smaller mass for the same drag force results in a larger deceleration. However, a larger drag coefficient would result in an earlier deceleration and more dissipation of energy prior to reaching the altitude of maximum g-load, which somewhat cancels the first order effect. Similarly, for the mass, a larger mass results in a deceleration starting later, and therefore a larger velocity at altitudes of maximum g-load, which somewhat cancels the first order reduction of $a/g$ from a larger mass (same force divided by a larger mass). This results in a relatively small change in the g-load with the ballistic parameter $K = \frac{mg}{C_D S}$, as seen in Figure 6a (up to 0.7% for a 20% change of each parameter). This is also shown by the analytical model from Equation (2). However, the altitude of the maximum deceleration does vary with m and $C_D$, as becomes obvious from the reasoning above: a larger mass dives deeper in the atmosphere before a significant deceleration kicks off, resulting in a shift down of the g-load profile, and a lower altitude for the maximum deceleration load. Inversely, a larger $C_D$ kicks off a significant deceleration earlier in the entry, shifting the g-load profile up. This is also shown in Equation (3), in a way that a decrease in K results in a higher altitude for the maximum g-load.

Following, the heat flux has a pronounced variation from changes in the mass and drag coefficient. On the one hand, an increased mass results in a larger heat flux (see Figure 6b), which can be linked to the kinetic energy of the vehicle. A more massive vehicle with a given entry velocity has a larger kinetic energy which is dissipated from the interaction with the atmosphere, translating into the thermal flux. Additionally, a larger mass will reach a lower altitude before getting significantly decelerated, meaning that the vehicle still has a relatively large velocity in denser regions of the atmosphere, which translates to a larger maximum aerothermal flux (and a lower altitude for this maximum). The effect of the drag coefficient is essentially the opposite of the mass: a $C_D$ permits the deceleration to start in higher layers of the atmosphere, dissipating more kinetic energy before the lower and denser altitudes are reached. This results in a decrease in the maximum $q_c$ and an increase in its related altitude. Those effects are also directly present in the analytical model shown by Equations (4) and (5).

It can be concluded from this analysis that the mass and drag coefficient of the vehicle are intrinsically related and have inverse effects on the thermo-mechanical loads acting on the vehicle. It is then more natural to consider the ballistic coefficient $K = \frac{mg}{C_D S}$, and its impact on the loads rather than the m and $C_D$ separately. A larger ballistic coefficient is desirable to reduce the g-load on the structure, however, it also results in a larger thermal flux. However, the parameter has no impact on the altitude difference between the two types of maximum in thermo-mechanical loads. When it comes to the design of an entry vehicle, trade-offs need to be performed between the structural and thermal subsystems to be able to handle the thermo-mechanical loads. As an example, if the heat shield is very capable, it might be desired to increase the ballistic parameter to reduce the mechanical load on the vehicle.